Evaluation of Whole-Body Vibration and Ride Comfort in a Passenger Car

Hassan Nahvi

Mechanical Eng. Dept., Isfahan University of Tech., Isfahan 84156-83111, Iran

Mohammad Hosseini Fouladi and Mohd Jailani Mohd Nor

MEMS-Automotive Research Group, Dept. of Mechanical and Materials Eng., Faculty of Engineering and Built Environment, Universiti Kebangsaan Malaysia, 43600 Bangi, Selangor, Malaysia

(Received 23 August 2008; revised 26 May 2009; accepted 11 June 2009)

Whole-body vibration transmission influences comfort, performance, and long-term health of the driver. This current study is an objective evaluation of vehicle comfort characteristics based on standard mathematical formulae and frequency analyses. A variety of road types were selected and quantified by using the International Roughness Index (IRI). To assess vibrations transmitted to the passengers, vibration dose values (VDV), kurtosis, frequency response functions (FRF), and power spectral densities (PSD) of the compartment recorded signals were evaluated. SEAT values based on VDV outputs qualified the seat suspension as a vibration isolator, whereas the FRF and PSD quantified that behaviour through frequency analyses. Results indicate that energy concentration is at frequencies lower than 30 Hz. Such low frequency excitations are well attenuated by seat suspension in the vertical direction but are amplified (up to five times in harsh conditions) by a backrest in the fore-aft trend. Signals are amplified beyond 30 Hz, but amplitudes are still very low. It seems that backrest assembly still can be improved to become a better isolator. However, T_{15} (time to reach severe discomfort), even in harsh conditions, is more than three hours, which exhibits the overall good quality of the vehicle suspension systems. Kurtosis and VDV correlate with IRI and may be used as two objective metrics, together with jury evaluation, to create a vehicle vibration-comfort index in the future.

1. INTRODUCTION

Vibration transmission to passengers has a large influence on comfort, performance, and health.[1] A comfortable ride is essential for a vehicle to obtain passenger satisfaction. Because of this, vehicle manufacturers are constantly seeking to improve vibration comfort. Many factors influence the transmission of vibration to and through the body. Transmission associated with the dynamic system depends on the frequency and direction of the input motion and the characteristics of the seat from which the vibration exposure is received. Vibrations up to 12 Hz affect all of the human organs, while those above 12 Hz have local effects.[2] Low-frequency (4-6 Hz) cyclic motions, like those caused by tires rolling over an uneven road, can resonate the body. Just one hour of seated vibration exposure may cause muscle fatigue and make the user more susceptible to back injury.

This paper is a subdivision of a general research conducted to evaluate vibro-acoustical comfort inside the vehicle compartment. The first part was to define a vehicle acoustical comfort index using objective and subjective evaluations.[3] This paper is an objective evaluation of vehicle vibration comfort, which is the first step of the vibration comfort assessment. Analysis of road conditions parameters, such as the International Roughness Index (IRI), and their correlation with kurtosis and the vibration dose value (VDV) can give useful information about the effect of road roughness on passenger vibration comfort.

Further research may include a subjective vibration evaluation (jury test), and the results of the subjective and objective assessments may be used to define an index for vehicle vibration comfort. This index eliminates the need for further subjective estimations and can be a useful parameter in various correlation analyses and vibration comfort predictions. It is believed that specific results of a vibration comfort index are only valid for the exact vehicle type. Still, different manufacturers can use the same method to derive the vibration comfort index for their products. Methods and general results of the current research (like correlations conducted for VDV, IRI, kurtosis, and velocity) are applicable for other researches as well.

Human responses to whole-body vibration can be evaluated by two main standards — the British Standard 6841 (BS 6841) (1987) and the International Standard 2631 (ISO 2631) (1997). The BS 6841 considers a frequency range of 0.5-80 Hz.[4] As shown in Fig. 1, this standard recommends measuring four axes of vibration on the seat (fore-aft, lateral, and vertical vibration on the seat surface as well as fore-aft vibration at the backrest) and combines them in an evaluation that assesses vibration severity. The ISO 2631 suggests vibration measurements in the three translational axes on the seat pan, but only the axis with the greatest vibration is used to estimate vibration severity.[5]

The current trend in vibration research is to use multi-axis values. This may be seen in studies (such as those by Paddan and Griffin[6] and Hinz et al.[7]). Huston and Zhao examined how the shape, frequency, and amplitude of mechanical shocks affect the comfort response of the seated human.[8] Recently, the effects caused by different experimental design variables on subjective response and vibration accelerations were investigated by Jonsson and Johansson.[9] In this study, ride comfort and vi-

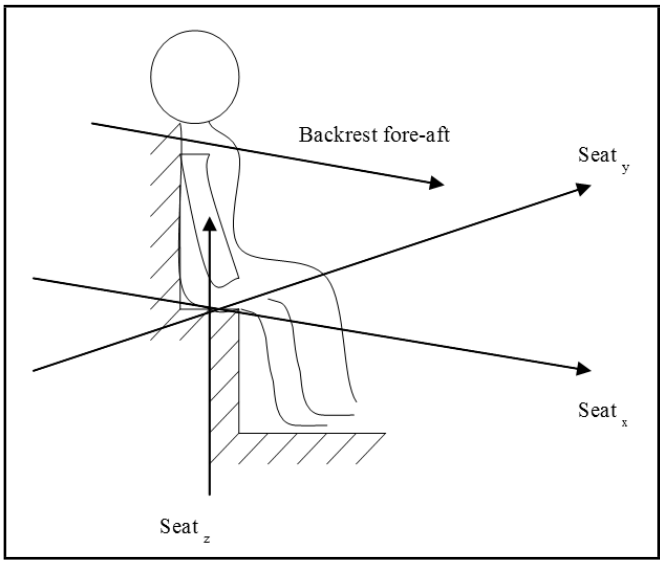

Figure 1. Schematic of four-axis vibration of a driver as considered by BS 6841.

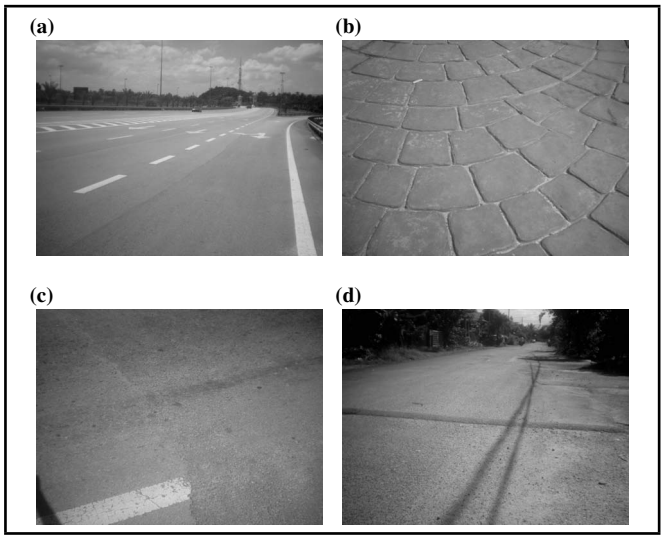

Figure 2. Road surfaces: (a) highway, (b) pavement, (c) suburban, and (d) bumpy.

Table 1. Characteristics of the road surfaces.

Location	Type	Characteristic
Seremban-Melaka	Highway	Smooth highway
Putrajaya Taman-Perdana	Pavement	Road consisting of small cobblestones
Kajang-UKM	Suburban	Poorly kept, rough country road
Kajang suburb	Bumpy	Road consisting of a series of bumps

bration characteristics of a passenger car were investigated at different vehicle speeds. The vehicle was driven over smooth and rough road surfaces.

2. EQUIPMENT AND PROCEDURE

The test vehicle was a mid-size Malaysian executive vehicle, Proton Perdana, with a V-6 engine. It is a four-door sedan with a curb weight of 1336 kg. With 16-inch rims and Lotus-tuned suspension settings, the car handles well through tight corners and is a good high-speed cruiser. The vibration signals were measured while driving over four flat road surfaces, and the speed was controlled manually by the driver. As shown in Fig. 2, the selected roads were highway, pavement, suburban, and bumpy. Characteristics of the road surfaces are presented in Table 1. The highway had a flat, smooth surface and occasional unevenness, which resulted in minimum disturbances. The pavement road was a cobbled street made by similar smooth stones with 5-mm thickness. The similar gap between the adjacent stones caused harmonic excitations with different periods at each axis. The suburban road had frequent random irregularities from 3 mm to 25 mm, which produced excessive casual vibration. The bumpy road was a suburban rough surface with high and sharp bumps up to 50 mm, which resulted in shock responses. The vehicle was driven at 20, 40, 60, and 80 km/h over all roads except the bumpy road. The driving speed over the bumpy road was only 20 km/h. The vehicle was also tested at 100 km/h on the highway.

Bruel and Kjaer instrumentation series (namely, portable and multi-channel analyser PULSE type 3560D, PULSE Labshop

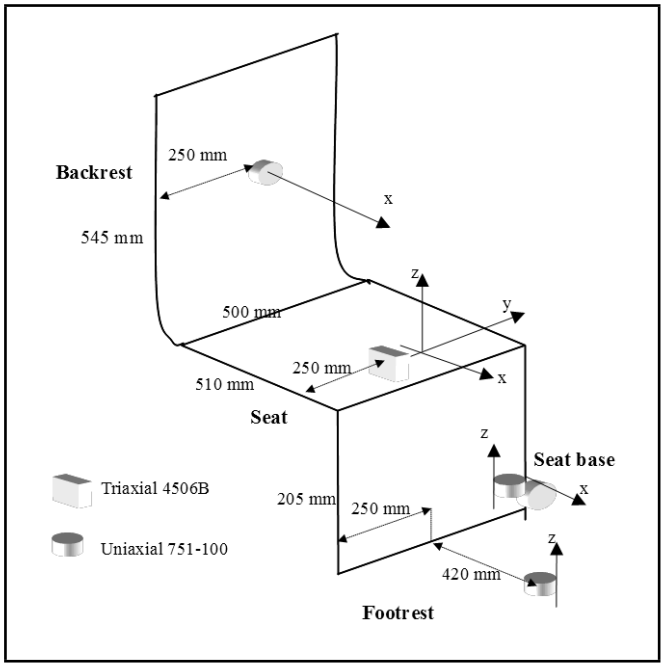

Figure 3. Schematic diagram of the experiment assembly and transducer mounting positions.

software with four ENDEVCO Isotron [uniaxial] accelerometers model 751-100 and B & K triaxial accelerometer type 4506B) were utilized in the measurement devices. The B & K calibration-exciter type 4294 was used to calibrate the accelerometers before and after the measurements. The dynamic frequency response of the uniaxial transducers was up to 10 kHz while that of the triaxial one was up to 5.5 kHz for the x axis and 3.0 kHz for the y and z axes. The sensitivity of both types of accelerometers was 10 mV/ms^{-2}.

A schematic diagram of the vehicle seat and accelerometer mounting positions is shown in Fig. 3. The triaxial accelerometer was mounted on the passenger seat surface (occupied by a torso) to measure vertical, fore-aft, and lateral accelerations. Vertical and fore-aft vibrations at the seat base were measured using two single-axis accelerometers placed on a rigid beam and mounted on the front, left seat rail. A similar mounting beam, containing a single-axis accelerometer, was attached on

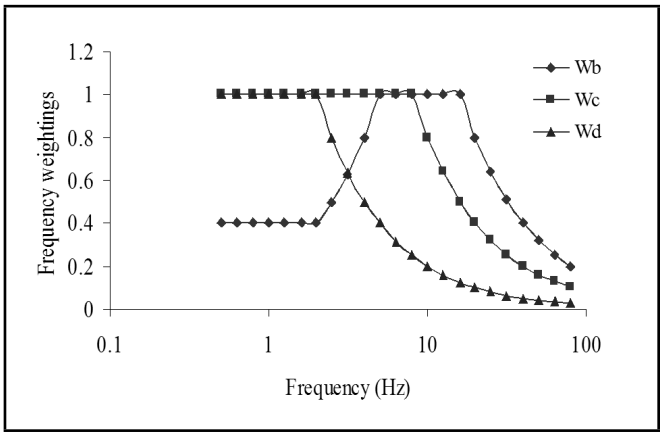

Figure 4. Frequency weightings used for the analysis of acceleration signals.[4]

the top of the backrest to measure fore-aft vibration. A single-axis accelerometer was placed on a plate and used to measure the vertical acceleration of the floor. It was mounted on the floor beneath the front edge and centreline of the seat. Signals were acquired into the 18-channel PULSE data-acquisition and analysis system. The signal-recording period was 60 s except when on the suburban road, which is mentioned in Section 4.4. According to the aforementioned standards, excitations up to 80 Hz should be counted for whole-body vibration analysis. Therefore, the frequency span of measurements was chosen as 100 Hz in the PULSE Labshop software. The sampling frequency was automatically adjusted to 256 Hz, according to the Nyquist rule (2.56 multiplied by 100 Hz as the frequency span). Signals were bandpass-filtered to be in the range of 0.5 to 80 Hz.

3. ANALYSIS

3.1. Frequency Analysis

Power spectral densities (PSD) were calculated for all acceleration signals. The power spectra show the distribution of energy across the frequency spectrum. Vibration evaluations were performed according to the recommendations in the BS 6841.[4] This involved the application of frequency weightings, multiplication of factors to allow for different sensitivity of the body in different axes, calculation of root-mean-square (rms) and VDV, and summation of values over different axes.

The acceleration was frequency-weighted using the frequency weightings defined in the BS 6841 over the frequency range 0.5 to 80 Hz. The three frequency weightings and multiplying factors for the different axes are listed in Table 2. The frequency-weighting values are shown in Fig. 4.

Table 2. Frequency weightings and multiplying factors as specified in the BS 6841 for a seated person.[4]

Location	Axis	Weighting	Multiplying factor
Seat	x	Wd	1.0
	y	Wd	1.0
	z	Wb	1.0
Backrest	X	Wc	0.8

3.2. Vibration Dose Values (VDV)

When the motion of a vehicle includes shocks or impulsive velocity changes, the VDV is considered more suitable for vibration assessment.[4,10] It gives a measure of the total exposure to vibration, taking into account the magnitude, frequency, and exposure duration. The VDV reflects the total, rather than the average, exposure to vibration over the measurement period and is considered more suitable when the vibration signal is not statistically stationary.[10] It is calculated by the fourth root of the integral with respect to the time of the fourth power of the acceleration after it has been weighted. The use of the fourth-power method makes the VDV more sensitive to peaks in the acceleration waveform. Intermittent vibration can be defined as interrupted periods of continuous or repeated periods of impulsive vibration, or continuous vibration that varies significantly in magnitude. Thus, the VDV ($\mathrm{ms}^{-1.75}$) is defined as

$$VDV = \left(\int_0^T a(t)^4 dt \right)^{1/4}, \quad (1)$$

where $a(t)$ is the frequency-weighted acceleration time history, and T is the period of time over which vibration occurs.[4,5] According to the BS 6841, vibration magnitudes and durations that produce VDV in the region of 15 $\mathrm{ms}^{-1.75}$ will usually cause severe discomfort. The exposure period required for the VDV to reach a tentative action level of 15 $\mathrm{ms}^{-1.75}$ can be calculated as

$$T_{15} = \left(\frac{15}{VDV_t} \right)^4 t, \quad (2)$$

where T_{15} is the time (in seconds) required to reach a VDV value of 15 $\mathrm{ms}^{-1.75}$, and VDV_t is the VDV measured over the period of t seconds. The VDV provide a suitable measurement of the total severity for whole-body vibration. According to BS 6841, excessive exposure to vibration may increase the risk of tissue damage in the body.[4] Basically, the VDV show the total amount of vibration received by the human over a period of time. Having this value shows the T_{15} level as the severe discomfort criteria. Hence, VDV and T_{15} determine the amount and the severity of vibration over a period of time.

3.3. Multi-Axis Vibration

The BS 6841 specifies that when evaluating multi-axis vibration, the fourth root of the sum of the fourth powers of the VDV in each axis should be determined to give the total vibration dose value, VDV_{total}, for the environment

$$VDV_{total} = (VDV_{xs}^4 + VDV_{ys}^4 + VDV_{zs}^4 + VDV_{xb}^4)^{1/4}, \quad (3)$$

where VDV_{xs}, VDV_{ys}, and VDV_{zs} are the VDV in the x, y, and z directions on the seat, respectively, and VDV_{xb} is the VDV in the x direction on the backrest.[4]

3.4. International Roughness Index (IRI)

Ride quality depends on vibration exposures induced by the road surface. IRI is the most common metric to describe road roughness. It is recognized as a general-purpose roughness index and is strongly correlated to most kinds of vehicle responses that are of interest.

Engineers use road profilers (road meter system) for IRI measurement. The key importance of IRI is that road profiler users have shared experiences measuring IRI. As shown in Fig. 5, it is a quarter (one corner) of the car system, which includes one tire and axle, suspension spring, and damper. It accumulates

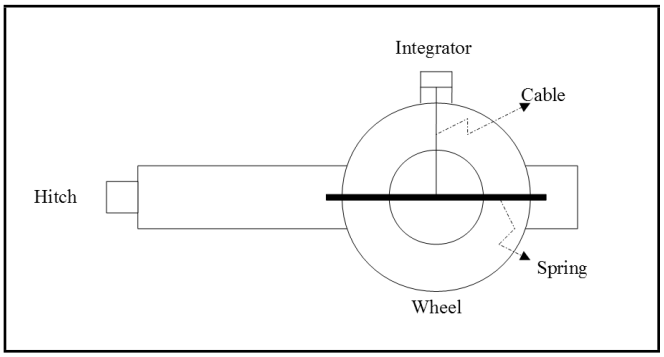

Figure 5. Schematic of a road profiler.

suspension motion while traveling over the road. Roughness is measured as the accumulated suspension stroke normalized by the total traveled distance. IRI is usually presented in engineering units such as mm/m, m/km, or inc/mile. It is highly correlated with acceleration of vehicle passengers (ride quality) and tire load (vehicle controllability).[11] Roads around the world may have different names and visual characteristics, but researchers can compare vibration analyses results for roads with similar IRI.

3.5. Kurtosis of Vibration Signals

Kurtosis is the fourth statistical moment signal, known as a global statistical parameter that is highly sensitive to the impulsiveness of the time-domain data. For discrete data sets it can be approximated by

$$K = \frac{1}{n\sigma^4}\sum_{j=1}^{n}(x_j - \bar{x})^4, \tag{4}$$

where K is kurtosis, n is the number of discrete data, σ is the standard deviation, x_j is any data, and $\bar{x}$ is the average of total data. The kurtosis value is approximately 3.0 for a Gaussian distribution. Higher kurtosis indicates the existence of numerous extreme data values, inconsistent with a Gaussian distribution, while lower than 3.0 designates a relatively flat distribution.[12]

3.6. SEAT Values

Seat comfort is usually assessed by making vibration measurements on the surface of the car seat based on the BS 6841. Seat-isolation performance was indicated by Seat Effective Amplitude Transmissibility (SEAT) values, which can be calculated from frequency-weighted rms accelerations on the seat surface and seat base, a_{seat} and a_{base}, respectively:[1]

$$SEAT_{rms}(\%) = \frac{a_{seat}}{a_{base}} \times 100. \tag{5}$$

Current standards recommend that if the input motion contains shocks, the *SEAT* value is determined using the VDV on the seat surface and seat base, VDV_{seat}, and VDV_{base} as[4,5]

$$SEAT_{vdv}(\%) = \frac{VDV_{seat}}{VDV_{base}} \times 100. \tag{6}$$

The SEAT value is a measure of how well the transmissibility of a seat is suited to the spectrum of entering vibration, taking into account the sensitivity of the seat occupant to different frequencies. SEAT values less than 100% indicate isolation or attenuation of vibration. It allows for the comparison of seat performance on a variety of road surfaces.[10]

4. RESULTS AND DISCUSSION

Figure 6 shows variations of VDV at different vehicle speeds over different roads except the bumpy road, where it was not possible to get data at different speeds. It may be seen that for each road surface, VDV values grew as the vehicle speed increased. At each speed, the measured VDV value over rough road surfaces (suburban and pavement) was greater than that over the smooth road (highway). The suburban road had the highest VDV increase in the speed range of 20 km/h to 40 km/h. As the vehicle speed increased, the smooth road surface showed a small VDV increase.

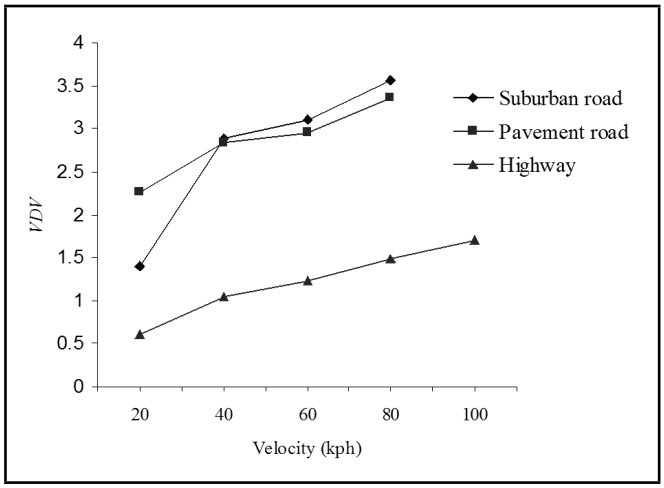

Figure 6. Variations of VDV values at different velocities over different roads.

Table 3. Time required to reach 15 $ms^{-1.75}$ VDV on rough road surfaces.

Road type	Velocity (km/h)			
	20	40	60	80
Pavement	32h 20m	12h 50m	11h	6h 15m
Suburban	219h	12h 10m	9h	5h 15m
Bumpy	3h 45m	-	-	-

The required exposure periods for VDV_{total} on the rough road surfaces to reach the action level of 15 $ms^{-1.75}$ are listed in Table 3. On the smooth road, the needed time to reach 15 $ms^{-1.75}$ VDV is so long in all speeds that it is not feasible to suppose that a driver can continuously drive such a long period of time. Therefore, it can be concluded that factors other than seat and cabin ergonomics affect drivers' comfort while driving on well-maintained, smooth roads.

4.1. IRI Evaluation

In this study, IRI (mm/m) is approximately related to the vehicle speed as follows:

$$\frac{a_{floor}}{IRI} = 0.16\left(\frac{\nu}{80}\right)^2, \tag{7}$$

where a_{floor} is the frequency-weighted floor acceleration (rms) in the vertical direction and ν is the vehicle speed in km/h.[13] For each road, using frequency-weighted floor acceleration values given in Table 4, the IRIs are calculated at different velocities and then averaged.

Table 4. Frequency-weighted floor acceleration (ms^{-2}, rms) for different roads and velocities and their corresponding average IRI values.

Road type	Velocity (km/h)				Average IRI
	20	40	60	80	
Highway	0.14	0.24	0.30	0.35	2.08
Pavement	0.5	0.65	0.71	0.8	5.46
Suburban	0.51	1.0	1.08	1.3	8.65
Bumpy	0.78	-	-	-	9.75

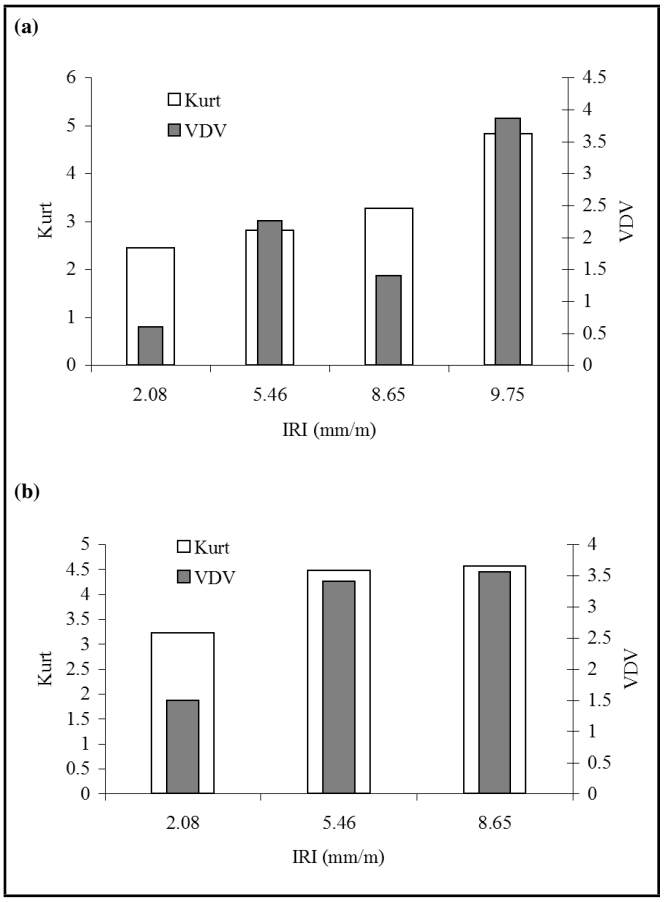

Figure 7. Variations of kurtosis and VDV versus IRI values: (a) 20 km/h and (b) 80 km/h.

4.2. Kurtosis Evaluation

To investigate whether the random vibration signals were Gaussian, a kurtosis parameter of the z-axis frequency-weighted floor accelerations were evaluated for different road surfaces at 20 km/h and 80 km/h.

Figure 7a shows the variations of kurtosis and VDV with changes in IRI (from Table 4) at 20 km/h. The right axis of each graph corresponds to VDV. It can be seen that kurtosis values increase as the IRI increases. This indicates a deviation of the acceleration signals from the Gaussian distribution as the IRI increases. On all the roads, VDV values increased as the road roughness increased. As expected, driving on rough road surfaces induces higher peaks and impulses. This resulted in more kurtosis and VDV values and less objective driver comfort. Hence, road roughness could be compensated through slowing down and thereby improving the ride quality. Similar results may be concluded from Fig. 7b, which shows variations of kurtosis and VDV versus road roughness at 80 km/h.

4.3. SEAT Values Evaluation

Figure 8 shows the comparison of VDV_{seat} and VDV_{base} for driving over road surfaces at specified speeds. Data points lie under a 45-degree diagonal starting at the origin. It shows SEAT values of less than 100% and isolation of vibrations.

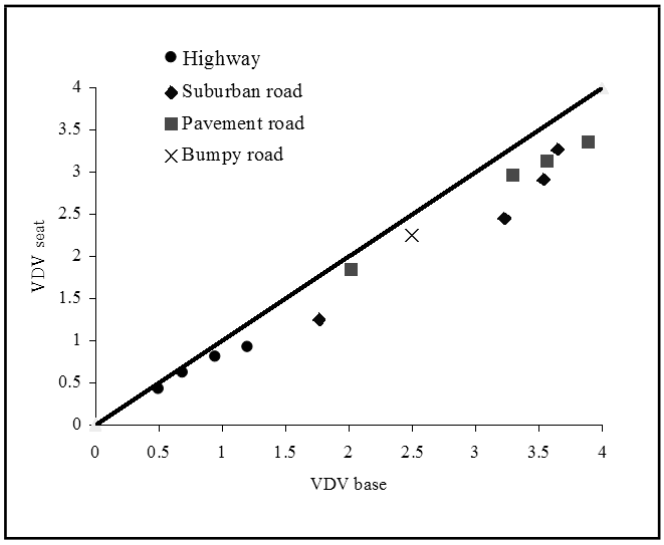

Figure 8. Comparison of the VDV_{seat} and VDV_{base} values on road surfaces.

4.4. Frequency Analysis of Vibration Signals

All signals (except on the suburban road) were acquired over a period of 60 s, and the frequency span of analysis was 100 Hz. The PULSE analyzer was adjusted in a way that an arbitrary number of 3200 lines were implemented in Fast Fourier Transform (FFT) analysis to achieve a high-frequency resolution of 31.25 mHz (100/3200).

The analyzer automatically detected the mean square of each signal and divided it by the bandwidth to calculate the PSD value. Such narrowband analysis shows high coherency, close to unity, between seat-surface and seat-base signals. The Frequency Response Function (FRF) analysis between these signals for the pavement road, at a speed of 20 km/h, is presented in Fig. 9. This graph implies that the seat structure was a good isolator of vibration below 30 Hz, while after that, the signal was amplified, but it was not a critical issue because, as shown

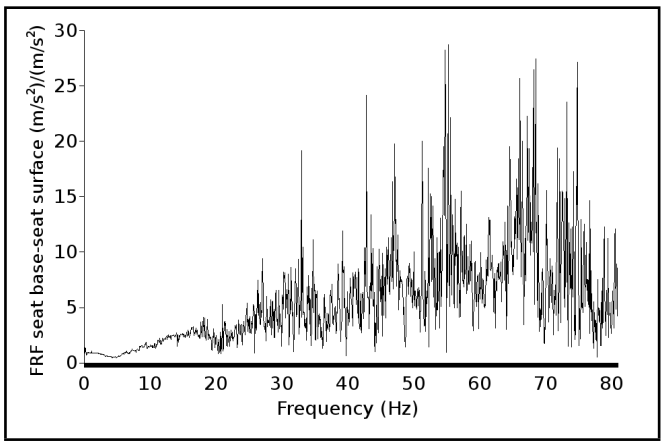

Figure 9. FRF between seat base and seat-surface signals while driving on the pavement road at 20 km/h.

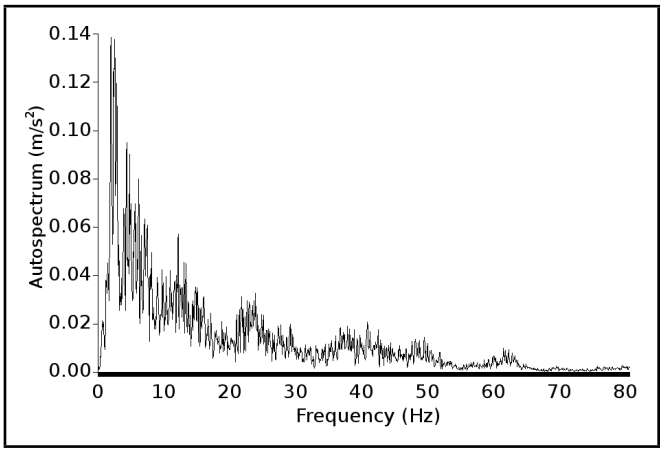

Figure 10. Autospectrum of the seat-surface vibration signal while driving on the pavement road at 20 km/h.

in Fig. 10, the amplitude of the signal after 30 Hz was still very low and had little effect on the passenger.

For the suburban road, in order to ensure similar conditions and better repeatability of results, a limited length of the road with the aforementioned characteristics was selected. The acquisition period varied from 20 s at 20 km/h to 3 s at 80 km/h, considering the road-length limitation. Therefore, to have the signal at the FFT analyzer output, the number of FFT lines was adjusted from 1600 lines at 20 km/h to 200 lines at 80 km/h with an equal frequency span of 100 Hz. Thus, the frequency resolution was 62.5 mHz at 20 km/h (100/1600) and 500 mHz at 80 km/h (100/200). The PSD of the vertical and fore-aft direction data that were measured on the seat surface and seat base while driving at 20 km/h on the suburban road are shown in Fig. 11. This figure shows how the accelerations at the base and seat surface were distributed over the frequency range up to 80 Hz. In the vertical direction, the measured acceleration on the seat surface (Fig. 11a) was comparable to the acceleration on the base (Fig. 11b). Base excitations were attenuated by the seat-isolation system up to 30 Hz. Accelerations were amplified at frequencies beyond that, but the magnitudes were very low.

However, acceleration on the base (Fig. 11d) was amplified in the fore-aft direction up to 30 Hz. Base vertical and fore-aft accelerations were mostly in the range below 30 Hz, which indicates a concentration of energy at low frequencies.

Figure 12 shows the PSD of vertical and fore-aft vibration data while driving on the suburban road at 80 km/h. Similar results may be seen in Fig. 12. On the seat surface in the vertical direction, the energy distribution tends to be concentrated toward the higher frequencies. Amplification of the fore-aft signal is achieved in low frequencies. This kind of energy observation is a powerful tool to check the capabilities of seat structures in the early stages of design, even on the test rig.

5. CONCLUSIONS

The IRI values (road roughness) indicate that the current study covered a wide variety of typical roads, ensuring that outputs are valid at different conditions. The study locations range from a highway, with an IRI value as low as 2.08, to a bumpy road, with an IRI value as high as 9.75. The kurtosis value increases with the IRI, which shows a deviation of the acceleration signals from the Gaussian distribution at higher IRIs.

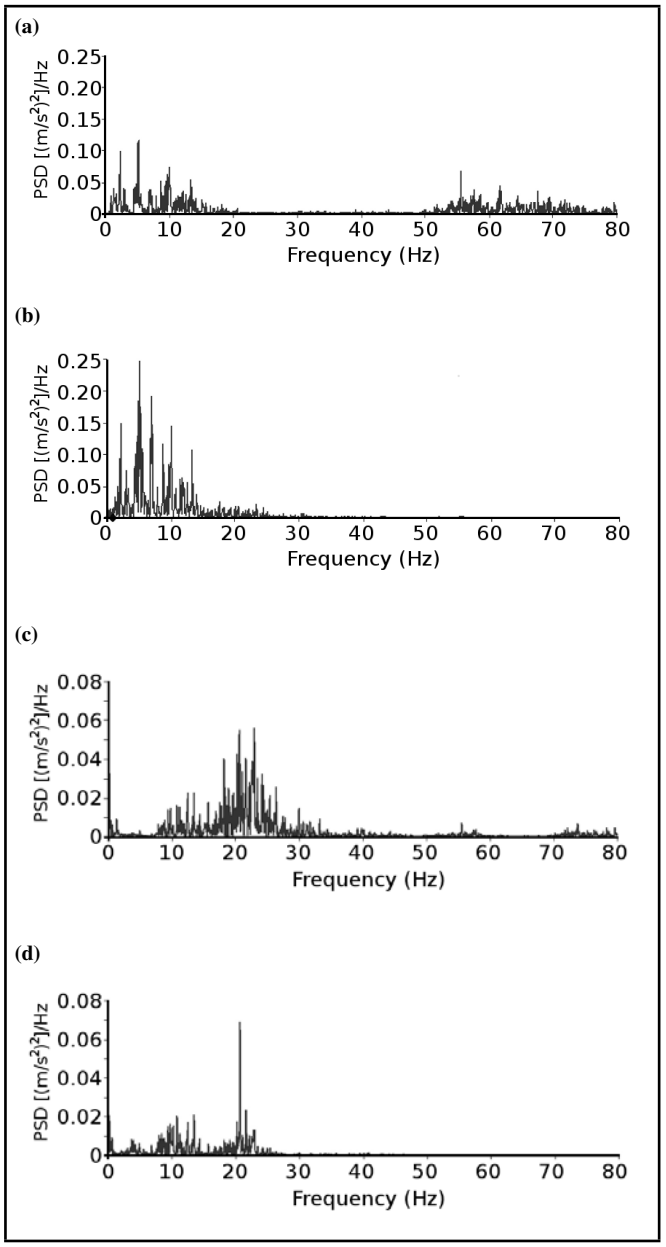

Figure 11. PSD of vibration data measured at the seat surface and base while driving on the suburban road at 20 km/h: (a) seat vertical direction, (b) base vertical direction, (c) seat fore-aft direction, and (d) base fore-aft direction.

The VDV (Vibration Dose Values) are proportional to both vehicle speed and IRI. Rough roads exhibit higher VDV variation as the vehicle speed changes. In other words, differentiation of the VDV with respect to speed is higher on harsh road conditions. The comparison of VDV values at seat surface and base (SEAT value) is a qualitative inspection of seat suspension, and it verified the isolation of vibration. Further frequency analysis gives deeper insight into the matter. The FRF (Frequency Response Function) is the transfer function between the seat base and surface, and it shows that excitations are damped up to 30 Hz by the seat and amplified beyond that range (in the vertical direction). The autospectrum of the seat-surface signal indicates that vibrations have low amplitudes even after amplifications at frequencies higher than 30 Hz. Generally, graphs show that energy concentration is at low frequencies — below 30 Hz. At the backrest in the fore-aft direction, excitations were amplified up to five times in severe conditions of driving at a high speed on a rough surface. Therefore, backrest

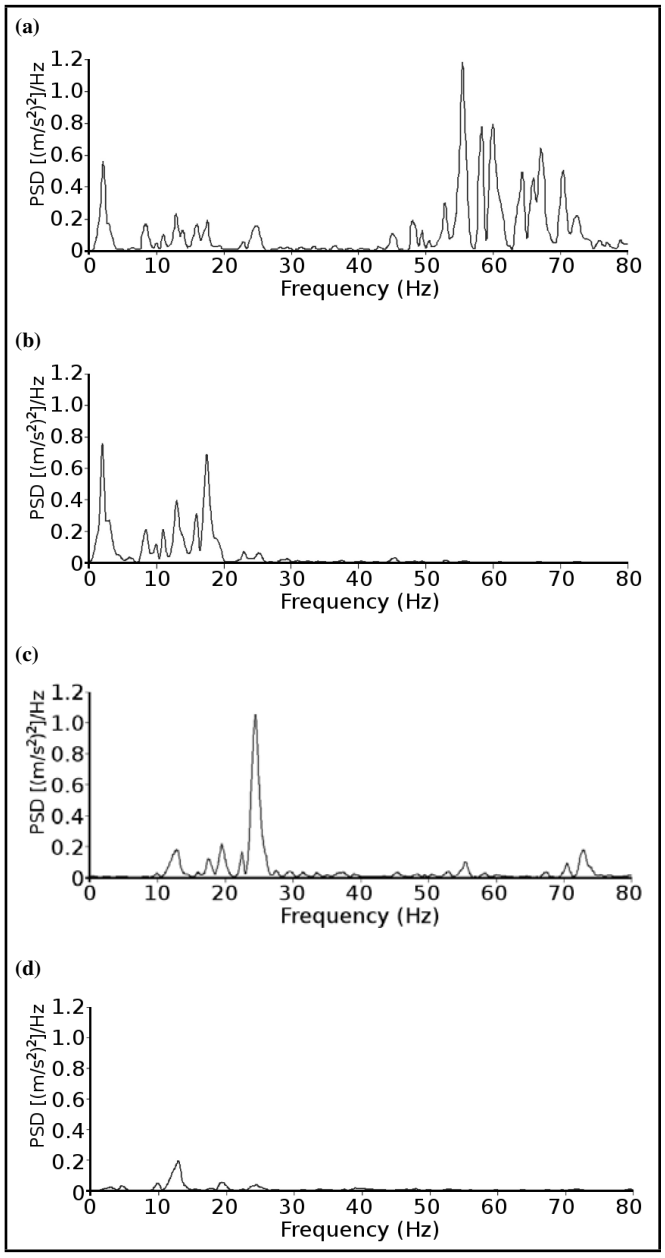

Figure 12. PSD of vibration data measured at the seat surface and base while driving on the suburban road at 80 km/h: (a) seat vertical direction, (b) base vertical direction, (c) seat fore-aft direction, and (d) base fore-aft direction.

assembly can still be improved to become a better isolator in this direction. However, the T_{15} value, even on an extremely harsh road condition (i.e., the bumpy road), was more than three hours suggests overall good quality of the vehicle suspension system and seat isolation. Finally, this study shows that kurtosis and the VDV of vibration signals correlate with the IRI and may be used as two objective metrics for vibration comfort estimation.

Acknowledgements

This study was conducted with support from IUT and UKM while Dr. H. Nahvi was on sabbatical leave from IUT. The first author would like to acknowledge the automotive laboratory facilities provided by the Department of Mechanical and Materials Eng., Faculty of Eng., UKM, Malaysia.

REFERENCES

[1] Griffin, M. J. *Handbook of Human Vibration*, Academic Press, London, (1990).

[2] Hostens, I., Papaioannou, Y., Spaepen, A., and Ramon. H. A study of vibration characteristics on a luxury wheelchair and a new prototype wheelchair, *Journal of Sound and Vibration*, **266**, 443–452, (2003).

[3] Nor, M. J. M., Hosseini Fouladi, M., Nahvi, H. and Ariffin, A. K. Index for Vehicle Acoustical Comfort Inside a Passenger Car, *Applied Acoustics*, **69** (4), 343–353, (2008).

[4] BRITISH STANDARDS INSTITUTION, BS 6841, Measurement and evaluation of human exposure to whole-body mechanical vibration and repeated shock (1987).

[5] INTERNATIONAL ORGANIZATION FOR STANDARDIZATION, ISO 2631, Mechanical vibration and shock — Evaluation of human exposure to whole-body vibration (1997).

[6] Paddan, G. S., and Griffin, M. J. Evaluation of whole-body vibration in vehicles, *J. of Sound and Vibration*, **253**, 195–213, (2002).

[7] Hinz, B., Seidel, H., Menzel, G., and Bluthner, R. Effects related to random whole-body vibration and posture on a suspended seat with and without backrest. *J. of Sound and Vibration*, **253**, 265–82, (2002).

[8] Huston, D. R. and Zhao, X. Whole-body shock and vibration: Frequency and amplitude dependence of comfort, *J. of Sound and Vibration*, **230**, 964–970, (2000).

[9] Jonsson, P. and Johansson, O. Prediction of vehicle discomfort from transient vibrations, *J. of Sound and Vibration*, **282**, 1043–1064, (2005).

[10] Paddan, G. S. and Griffin, M. J. Effects of seating on exposures to whole-body vibrations in vehicles, *J. of Sound and Vibration*, **253** (1), 215–241, (2002).

[11] Sayers, M. W. and Karamihas, S. M. *The Little Book of Profiling*, Regent of the University of Michigan, (1998).

[12] Bendat, J. S. and Piersol, A. G. *Random Data: Analysis and Measurement Procedures*, Wiley-Interscience, New York, (1971).

[13] Ahlin, K. and Granlund, J. International Roughness Index, *IRI*, and ISO 2631 vibration evaluation, Technical paper, Transportation Research Board, Washington D C, (2001).

On Active Noise Reduction in a Cylindrical Duct with Flow

Louis M. B. C. Campos and Fernando J. P. Lau

Centro de Ciências e Tecnologias Aeronáuticas e Espaciais (CCTAE), Instituto Superior Técnico, 1049-001 Lisboa, Portugal.

(Received 30 December 2008; accepted 27 April 2009)

An analytical approach to active-noise reduction is presented in the case of a line-source in a cylindrical enclosure, minimizing the noise in a sector, corresponding to (i) the passenger head area of an aircraft cabin for a cylindrical fuselage, in the absence of flow, and (ii) a sector or an annulus of noise reduction outside of a cylindrical duct carrying a uniform axial flow of an arbitrary Mach number. In both cases, the noise is assumed to consist of the superposition of modes, and the anti-noise is used to cancel the fundamental mode and/or specified harmonics. The total acoustic energy in the region of interest is calculated for the residual and original sound field, and their ratio specifies the noise-reduction function. The latter is minimized by adjusting the source position, and the noise reduction achieved is plotted versus the dimensionless radial wave number, taking into account mean flow effects. The case of the original noise field, consisting of the fundamental and the anti-noise source set to cancel this, is taken as the baseline for further comparison. Cases with several anti-noise line-sources set to cancel various combinations of the fundamental and harmonics are also considered; for example n anti-noise sources are used to cancel the fundamental and first n-1 harmonics. For a given noise field, the improvement in noise-reduction performance with the number of anti-noise sources is demonstrated, both for cylindrical and planar enclosures. The addition of anti-noise sources while reducing noise at low frequencies can cause an increase in noise at high frequencies; the latter may be countered by passive means. All results obtained follow from the calculation of the noise-reduction function in terms of Bessel functions, which can be evaluated with their zeros, using asymptotic methods, which are shown to be reasonably accurate.

1. INTRODUCTION

One of the major areas of classical acoustics[1–4] concerns sound propagation in ducts, of uniform or varying cross-section, i.e., horns,[5–9] with or without mean flow, i.e., nozzles.[10–19] The recent interest on active-noise reduction naturally focused on duct acoustics like propeller noise suppression in an aircraft fuselage;[20–23] this is one aspect, viz. discrete tone suppression, of active-noise reduction in enclosures, which may also involve active suppression of structural vibration.[24–27] Active-noise reduction has also been considered for sound in nozzles,[28,29] although it is more often applied to structural acoustics.[30–33] Thus, active-noise reduction in nozzles has been much less researched than other aspects, such as propagation in sheared[10,11,34–37] or swirling[38–40] mean flow, effect of uniform[41–43] or non-uniform[44–47] wall impedance, and radiation from the nozzle exit across a vortex sheet[48,49] or turbulent and irregular shear layer.[50,51] The two main purposes of this paper are (i) to address active-noise reduction in a cylindrical duct with uniform axial flow, thus applying to nozzles, and as a particular non-flow case, to a cylindrical aircraft cabin; and (ii) to take analytical methods farther than usual, e.g., to calculate the noise reduction due to active-noise suppression in a closed form.

Active-noise reduction is considered (Section 2) in a cylinder for a given frequency and axial wave number and any superposition of radial and circumferential modes. The anti-noise source is taken to be (Section 2.1) a continuous, uniform, coherent line-source parallel to the axis of the cylinder (Fig. 1), whose position is arbitrary, i.e., it is specified by a distance from the axis and angle relative to the noise-reduction sector, which are subject to optimization (Fig. 2a). The criterion for optimization is (Section 2.2) the minimum total-acoustic energy in a circular sector (Fig. 2b) simulating the passenger head area or volume in an aircraft; in the case of a nozzle, the noise reduction may be considered over an angular sector if sound transmission is more sensitive in a particular direction. If sound transmission in all directions is of concern, the angular sector, which has arbitrary aperture, can be extended to a circular annulus. The calculations are explicitly made first for a noise field consisting only of a fundamental mode; the same method applied to any harmonic, and by linear superposition, to any combination of fundamentals and harmonics. A single anti-noise source may be tuned to cancel the fundamental or any harmonic. Using several anti-noise sources, the fundamental and several harmonics can be cancelled simultaneously. Even for a noise field consisting only of one mode, e.g., the fundamental and one anti-noise source tuned to cancel the fundamental, the anti-noise source also generates harmonics, and these will appear in the residual noise field.

In general, the residual noise field (Section 2.2) will be represented by a double series of radial plus circumferential harmonics, without some terms corresponding to cancelled modes; the associated acoustic-energy density is quadratic in the acoustic pressure, and thus, is specified by a four-fold series. The integration over the whole cross-section of the cylinder would considerably simplify the series, because the eigenfunctions are orthogonal; they are not orthogonal in the noise-reduction area of interest, and thus, the reduction from a four-fold to a single series is the main mathematical challenge. The noise-reduction function is defined as the ratio of